A PS-SWM Strategy for Isolated Modular Multilevel DC/DC Converter with Reduced Passive Component Size and Low Total Device Rating

Ran Mo, Ren Xie, Yanjun Shi, Hui Li
Center for Advanced Power Systems
Florida State University
Tallahassee, FL, USA
hli@caps.fsu.edu

***Abstract*—The isolated modular multilevel dc/dc converter (IM2DC) based on modular multilevel converter (MMC) is a promising dc/dc power conversion topology in HVDC/MVDC applications. In this paper, a novel phase-shifted square wave modulation strategy (PS-SWM) is proposed for IM2DC. Compared to the conventional modulation methods, the proposed technique achieves a smaller dc inductance due to higher equivalent switching frequency. In addition, the required capacitor energy can be reduced, which decreases the capacitor size without total device rating (TDR) penalty. The operation principles of the proposed method are presented. The passive components are designed and compared with those using other modulation methods. The experimental results are provided to validate the proposed modulation strategy.**

Keywords—phase-shifted square wave modulation; isolated modular multilevel dc/dc converter; passive components design

I. INTRODUCTION

The dc/dc converters play an essential role for flexible power exchange and voltage regulation in HVDC/MVDC grids. The isolated modular multilevel dc/dc converter (IM2DC), which consists of two modular multilevel converters(MMC) connected through a medium-frequency transformer, provides the solution to dc/dc conversion with low-rating devices, superior fault performance and lower cost in HVDC/MVDC systems[1-6].

Various modulation methodologies have been proposed in IM2DC with distinct advantages. The phase-shifted (PS) sinusoidal modulation, which is widely applied in traditional MMCs with high quality ac output, can be used in IM2DC directly[2-3]. Compared to the sinusoidal modulation, the two-level (2L) modulation generates a square wave ac-link voltage, which leads to a higher efficient power transfer capability[4]. Recently a quasi two-level (Q2L) modulation has been proposed for not only lower *dv/dt* but also soft-switching capability[1][5]. In addition, triangular modulation is discussed as well which exhibits lower harmonic components than 2L modualtion and simpler implementation than sinusoidal modulation[6].

On the other hand, the IM2DC arm voltage and current vary with the same delivered power via different modulations, which affects both the total device rating (TDR) and passive component sizes. Large cell capacitors are needed for sinusoidal modulation. Meanwhile, triangular modulation results in large arm RMS current leading to a higher TDR and conduction loss. With 2L and Q2L modulation, smaller capacitors and devices are applicable, however, the dc current ripples of dc inductors may be larger than those using multi-cell phase-shifted modulation method.

This paper proposes a novel phase-shifted square wave modulation (PS-SWM) strategy to reduce the passive components size without TDR penalty. Compared to the conventional modulations, the PS-SWM requires smaller cell capacitors and dc inductors at the same time. Furthermore, a high efficient power transfer capability of the 2L modulation and low TDR of Q2L modualtion can be achieved in the proposed PS-SWM method. Section II introduces the operation principle of proposed PS-SWM. The design of passive components are presented in Section III. The comparisons with other modulations reveal the benefits of proposed PS-SWM. The experimental verifications are demonstrated in Section IV. Section V is the conclusion.

II. PROPOSED PHASE-SHIFTED SQUARE WAVE MODULATION (PS-SWM)

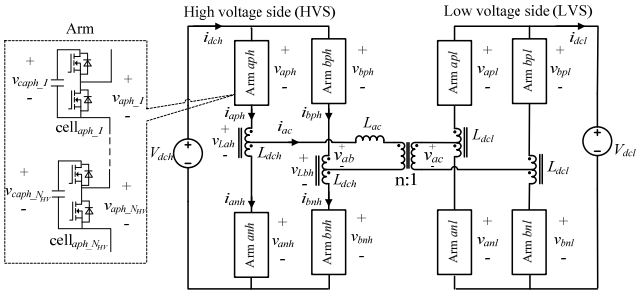

Fig. 1. The topology of IM2DC.

Fig.1 demonstrates the topology of IM2DC consisting of two single-phase MMCs connected through a medium-frequency transformer, where half-bridge cells are cascaded

This work was sponsored by the US Office of Naval Research under contract N000141612956.

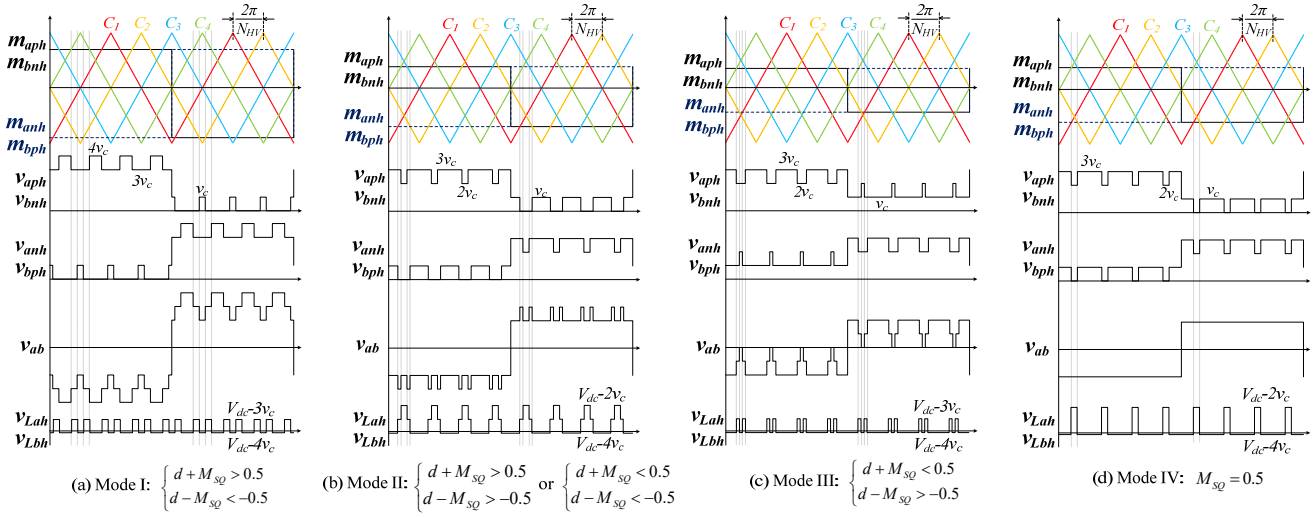

Fig.2.The operation modes and the corresponding waveforms of PS-SWM: modulation waveforms, arm voltage, ac voltage and dc inductor voltage when $N_{HV}=4$.

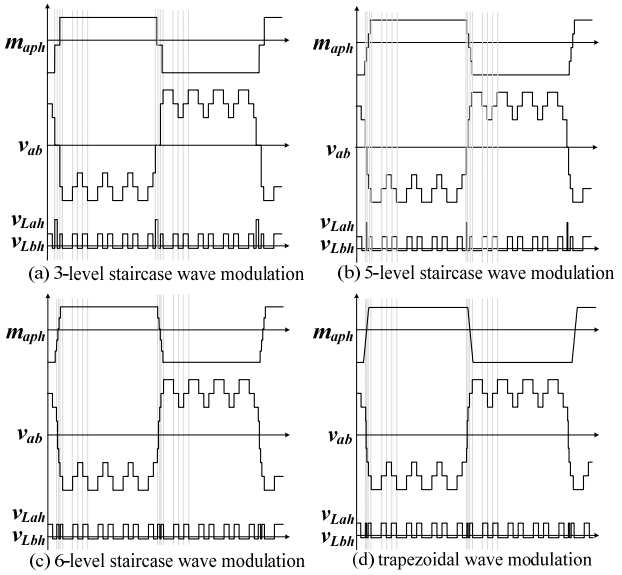

Fig.3. The ac voltage and dc inductor voltage waveforms with different modulation waveforms.

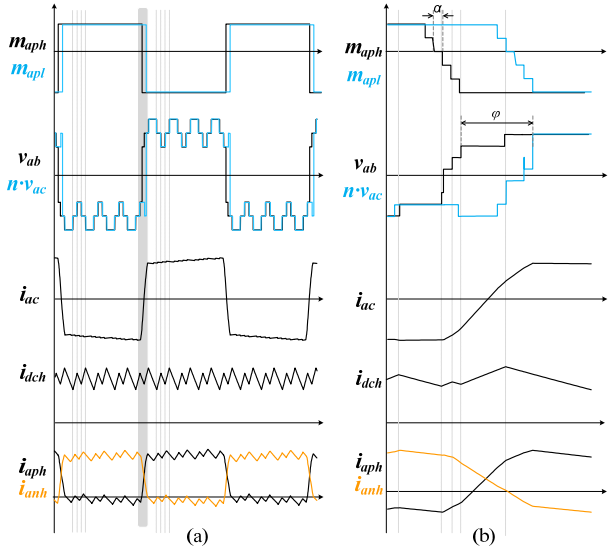

Fig.4. The key waveforms of IM2DC with PS-SWM: (a) voltage and current; and (b) zoomed view of the shaded range in (a).

within each arm. Distributed cell capacitors are installed at the dc link of each cell and coupled arm inductors and one extra inductor are adopted as the dc and ac inductor respectively.

The high voltage side (HVS) waveforms of proposed PS-SWM strategy as well as the corresponding arm voltages and transformer voltage are illustrated in Fig.2, where four cells within one arm is selected as an example. A square waveform with 0.5 duty cycle is adopted as the modulation waveform, where magnitude M_{SQ} and dc offset d are controllable. $m_{a(b)ph}$ and $m_{a(b)nh}$ of Fig.2 are the modulation waveforms of phase *a (b)* upper arm and lower arm respectively. N_{HV} is the HVS cell number in one arm, which is 4 in this example, C_1~C_4 are carrier waveforms. m_{aph} is the same as m_{bnh}, which is 180° phase-shifted with the m_{anh} and m_{bph}. A phase-shifted angle $2\pi/N_{HV}$, is applied among C_1~C_4, which increases the equivalent switching frequency. As shown in Fig.2, when the square modulation waveform varies with different M_{SQ} and d, the generated arm voltage v_{xyh} (x = a, b; y = p, n) and ac voltage v_{ab} changes accordingly, resulting in four different operation modes. Among these operation modes, Fig.2 (a) is considered as the desired mode with largest modulation index since v_{ab} can be as high as dc bus voltage V_{dch}, which achieves lowest converter TDR. This will be explained in the next section.In addition, the highest voltage ripple frequency and lowest ripple magnitude occur at the same time on the dc inductor voltage v_{Lah} and v_{Lbh} in this mode, which indicates the smallest inductor size can be achieved. It is worth mentioning that the phase-shifted angle can also be π/N_{HV} among the

carriers in one phase. Consequently, it is possible to reduce the dc inductor further.

A staircase or trapezoidal modulation waveform instead of a square wave can be utilized to reduce the ac voltage *dv*/*dt*, Fig.3 (a) ~ (d) demonstrates v_{ab} with different staircase and trapezoidal modulation waveforms. When the staircase level increases, v_{ab} has more levels and smaller *dv*/*dt*, smaller dc current ripples can be obtained as well due to higher equivalent ripple frequency of v_{Lah} and v_{Lah}. Fig.3 also indicates that 6-level staircase wave modulation already attains the same ac voltage level with that of trapezoidal wave modulation, which is adequate for reduced *dv/dt* performance.

Fig.4 depicts the key waveforms considering both HVS and LVS with proposed modulation method. The operation principle of LVS is similar to that of HVS, but with a phase shift angle φ to transfer the power. Although the magnitude of modulation waveform can vary in the LVS as well, usually it equals to that of the HVS modulation waveform to ensure high efficiency. Similar to MMC, both dc bus current i_{dch} and transformer current i_{ac} flow though the cells, therefore the arm current contains both dc and ac components as shown in Fig.4 using HVS phase a arm i_{aph} and i_{anh} as examples. Moreover, the small stair step angle α with acceptable *dv/dt* are preferred, otherwise the dc voltage utilization will be sacrificed. In this paper, this angle is assumed to be very small, such that they can be neglected in the following analysis.

III. TDR AND PASSIVE COMPONENTS DESIGN AND COMPARISON

A. TDR and passive components design

If considering the dc and ac components separately, the IM2DC HVS arm voltage and current can be written as in (1).

$$\begin{cases} v_{aph} = v_{bnh} = \dfrac{V_{dch}}{2} - \dfrac{v_{ab}}{2}, v_{bph} = v_{anh} = \dfrac{V_{dch}}{2} + \dfrac{v_{ab}}{2} \\ i_{aph} = i_{bnh} = \dfrac{i_{dch}}{2} + \dfrac{i_{ac}}{2}, i_{bph} = i_{anh} = \dfrac{i_{dch}}{2} - \dfrac{i_{ac}}{2} \end{cases} \quad (1)$$

If ignoring the stair step angle and the high frequency ripples, the ac voltage of IM2DC can be considered as a pure square wave as in (2):

$$v_{ab} = V_{ab} \cdot S[\theta], S[\theta] = \begin{cases} 1, \theta \in [0, \pi] \\ -1, \theta \in (\pi, 2\pi] \end{cases} \quad (2)$$

where the magnitude of the ac voltage, V_{ab}, is adjustable with proposed PS-SWM, which can be defined as

$$V_{ab} = k \cdot V_{dch} \quad (3)$$

where *k* is the voltage ratio of ac to dc.

The voltage and current stress of the device in HVS is:

$$v_s = \frac{V_{dch}}{2N_{HV}} + \frac{V_{ab}}{N_{HV}}, i_s = \frac{i_{dch}}{2} + \frac{i_{ac}}{2} \quad (4)$$

Then the TDR with PS-SWM in IM2DC HVS can be calculated as in (5), where *P* is the power rating of IM2DC.

$$\begin{aligned} TDR_{HVS} &= 4N_{HV} \cdot \left(\frac{V_{dch}}{2N_{HV}} + \frac{V_{ab}}{2N_{HV}} \right) \cdot \sqrt{\left(\frac{i_{dch}}{2} \right)^2 + \left(\frac{i_{ac}}{2} \right)^2} \\ &= P \cdot (1+k) \cdot \sqrt{1 + \frac{1}{k^2}} \end{aligned} \quad (5)$$

Based on (5), the smallest TDR can be accomplished when the ac voltage magnitude equals to dc bus voltage, i.e, $k = 1$. Similar analysis can be applied to the LVS as well, hence the TDR of IM2DC with PS-SWM is derived as in (6):

$$TDR_{IM2DC} = 4\sqrt{2} \cdot P \quad (6)$$

The cell capacitors in IM2DC serve as the energy buffer between dc and ac terminal, which handle the maximum energy variation over one fundamental cycle. The cell capacitor size are determined to limit the capacitor voltage ripples and derived as in (7):

$$N_{HV} \cdot C_{HV} \cdot V_C^2 \cdot \sigma = \Delta E_{\max} \quad (7)$$

C_{HV} denotes the HVS cell capacitance, V_C is the nominal capacitor voltage and σ is the peak-peak capacitor voltage ripple percentage. Due to the similarity, only the design of HVS passive components is presented.

Based on (1) and (3), the instantaneous energy stored in one arm is calculated as:

$$E_{arm} = \int \frac{1}{4} P \cdot \left(k - \frac{1}{k} \right) \cdot S[\theta] dt \quad (8)$$

According to the aforementioned analysis, IM2DC is desired to operate at $k = 1$. As a result, there will be no low frequency ripple components existing in the capacitors. Therefore, the cell capacitors can be much smaller since they are dedicated to smooth the switching frequency ripples only. Thus the capacitor can be approximately sized as

$$\begin{aligned} C_{HV} &= \left(\frac{I_{dch}}{2} + \frac{I_{ac}}{2} \right) \cdot \frac{1}{\sigma \cdot V_C} \left[\frac{\pi (d - M_{SQ} + 1)}{\omega} + \frac{|\varphi|}{2\omega_{tr}} \right] \\ &\approx \frac{I_{dch}}{\sigma \cdot V_C} \left[\frac{\pi |d|}{\omega} + \frac{|\varphi|}{2\omega_{tr}} \right] \end{aligned} \quad (9)$$

where ω and ω_{tr} are the angular cell switching frequency and transformer frequency respectively, and I_{dch} is the nominal dc current.

The dc inductor is designed to suppress the dc current ripple. As can be seen from Fig.2 (a), the equivalent dc current ripple is $2 \cdot N_{HV}$ times of the cell switching frequency. The dc inductor can be calculated by (10), where γ is the peak-peak dc current ripple percentage and L_{dch} is the HVS dc inductance.

$$L_{dch} = \frac{2\pi \cdot V_{dch}}{\omega \cdot N_{HV} \cdot \gamma \cdot I_{dch}} |d| \tag{10}$$

B. Comparsion with conventional modulation methods

The design results of TDR and passive components of IM2DC using different modulation methods are shown in Table I. The TDR of PS-SWM and Q2L [1] is 18% less than that of PS-sinusoidal modulation due to the higher efficient power transfer capability of square wave. The per unit value of total capacitor energy is used to compare the capacitor size. With PS-sinusoidal modulation, the cell capacitors have to withstand both the fundamental and double frequency energy variations [7]. Although the fundamental frequency voltage ripple can be eliminated by some methods to achieve smaller capacitors, those methods will result in higher TDR. On the other hand, the cell capacitor with Q2L[1] and proposed PS-SWM can be much smaller since only higher switching frequency ripple exists when k is 1. Although the required switching ripple energy using PS-SWM will be a little larger than the one using Q2L[1], other factors such as the loss and heat dissipation also need to be considered for capacitor sizing. Hence the cell capacitors using Q2L and PS-SWM will have similar size. Table I also gives the calculated dc inductors using Q2L[1] and PS-SWM when k is 1, which are both designed to limit the dc current switching ripple. Since 1-2D and $|d|$ will have similar values under same converter ratings, the dc inductor with PS-SWM will be approximately N_{HV} times smaller than that with Q2L. When PS-sinusoidal modulation is applied, not only the switching ripple current but also the double frequency circulating current I_{2ftr} need to be suppressed by the dc inductor [8], therefore the dc inductor will be largest.

TABLE I. COMPARISON OF IM2DC WITH DIFFERENT MODULATION METHODS

Parameters / Modulation	TDR/P	Total capacitor energy $J/KVA \cdot S^{-1}$	DC inductance
PS-sinusoidal	$4\sqrt{3}$	$\frac{3\sqrt{3}}{4\pi\sigma}$	$\frac{P/(4I_{2f_{tr}})+V_{dch}/2}{16\pi^2 f_{tr}^2 \cdot C_{HV} \cdot V_C}$
Q2L [1]	$4\sqrt{2}$	$\frac{\lvert\varphi\rvert}{\pi\sigma}$	$\frac{2\pi \cdot V_{dch} \cdot (1-2D)}{\omega \cdot \gamma \cdot I_{dch}}$ [b]
Proposed PS-SWM	$4\sqrt{2}$	$\frac{\lvert\varphi\rvert}{\pi\sigma} + \frac{2\lvert d\rvert}{\sigma} \cdot \frac{f_{tr}}{f}$ [a]	$\frac{2\pi \cdot V_{dch} \cdot \lvert d\rvert}{N_{HV} \cdot \omega \cdot \gamma \cdot I_{dch}}$

[a] f_{tr} and f are the transformer frequency and cell switching frequency respectively.

[b] D *is* the duty cycle [1].

IV. Experimental Verification

A downscaled prototype is built in the lab to verify the proposed modulation method. The experimental setup of 2kW IM2DC is shown in Fig.5. To present the multi-level characteristics, four cells are installed in each arm. Detailed circuit parameters are given in Table II. The fundamental frequency is selected as 10kHz to reduce the sizes of passive components. The switching frequency is designed at 40kHz to ensure the quality of ac terminal voltage. One side of IM2DC is built and connected to an R-L load, which is adequate for validating the proposed modulation. The open-loop control is applied in the converter with fixed square wave magnitude and dc offset.

TABLE II. CIRCUIT PARAMETERS OF THE IM2DC PROTOTYPE

Parameters	Specifications	Parameters	Specifications
Rated power P	2kW	Input voltage V_{dc}	250V
Cell number N	4	Cell capacitor C	20μF
DC inductor L_{dc}	100μH	AC inductor L_{ac}	17 μH
Switching frequency f	40kHz	AC frequency	10kHz
Cell MOSFETs	IRFP260N	Load resistor	10Ω

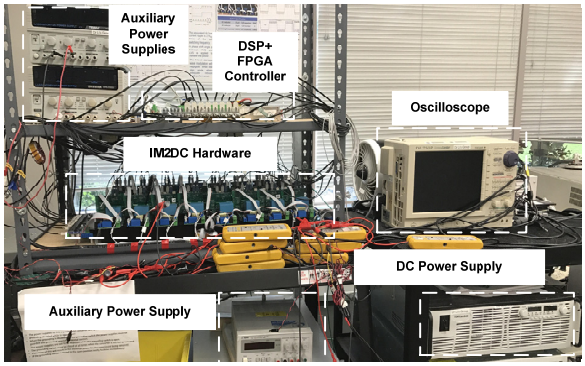

(a)

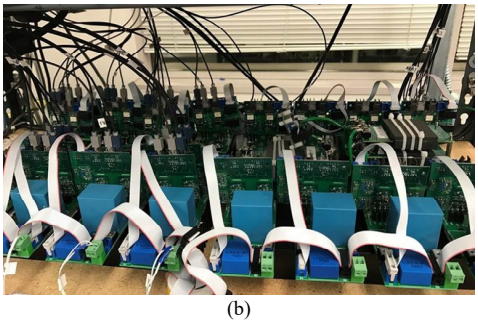

(b)

Fig.5 Experimental setup: (a) testbed setup; and (b) 2kW IM2DC protoytpe.

Fig.6 demonstrates the key waveforms of the IM2DC with proposed PS-SWM. The arm voltages $v_{a(b)p(n)}$ and ac terminal voltage v_{ab} are consistent with the theoretical analysis in Fig.2 (a), which exhibits the square wave shape with high equivalent switching frequency ripples at 160kHz in this scenario. The zoomed view of v_{ab} from Fig.6 (b) illustrates the multilevel characteristics of proposed modulation methods.

Fig.7 shows the key waveforms of the IM2DC with lower ac link dv/dt. A staircase wave is applied as the modulation

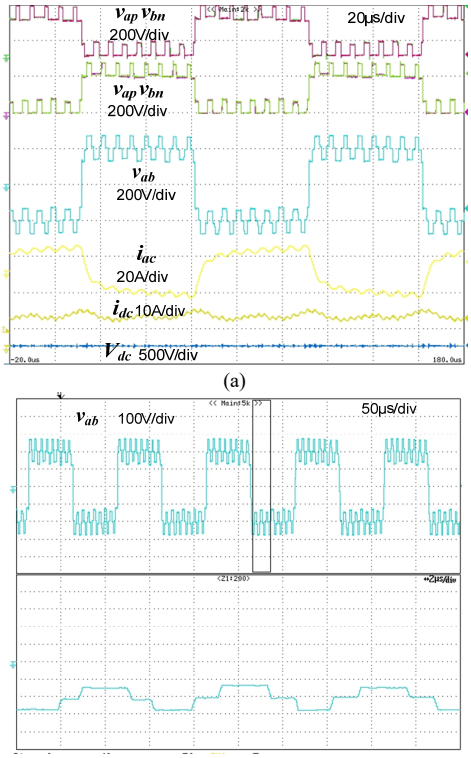

Fig.6 Experimental results of iM2DC with proposed PS-SWM: (a) key waveforms; and (b) multilevel features.

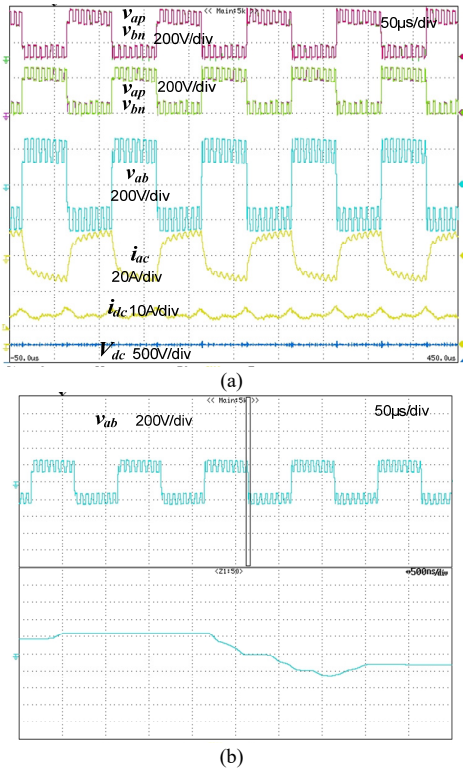

Fig.7 Experimental results of iM2DC with staircase wave modulation: (a) key waveforms; and (b) staircase features.

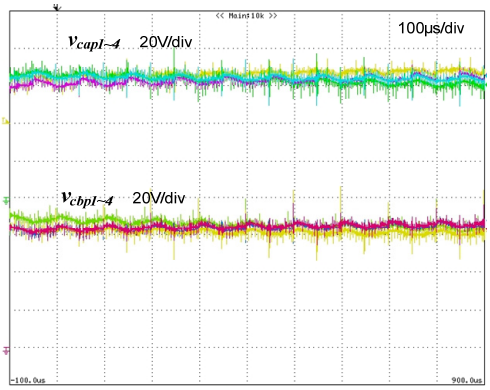

Fig.8 Experimental results of capacitor voltages in the upper arms.

waveform. Since stair step angle α is as small as 1.5°, it can be ignored in the power analysis. The zoomed view of v_{ab} from Fig.7 (b) presents the stair steps in the edges indicating a lower dv/dt compared to the pure square wave modulation.

Fig.8 shows the cell capacitor voltages in the upper arms *ap* and *bp*. It shows that the capacitor voltage maintains stable and balanced. A 10kHz fundamental frequency component exists because the ac to dc ratio k is 0.8 instead of 1. The cell capacitor voltages waveforms in the lower arms *an* and *bn* exhibit the same features as shown in Fig.8.

V. CONCLUSIONS

In this paper, a novel phase-shifted square wave modulation (PS-SWM) technique is proposed for IM2DC application in HVDC/MVDC systems. The detailed operation principles are explained and the converter passive components with PS-SWM as well as TDR are derived. The results show that the cell capacitor can be reduced significantly and lower TDR can be achieved compared to the conventional PS-sinusoidal method. Both Q2L and proposed PS-SWM can achieve low TDR and small cell capacitor size, however, the PS-SWM can allow smaller dc inductors due to the multi-cell phase-shifted characteristics. Although Q2L can realize soft-switching to reduce switching loss, the PS-SWM can achieve lower switching frequency if the cell number is large enough, therefore, the total device loss of PS-SWM is comparable with that of Q2L.

REFERENCES

[1] Y. Shi, and H. Li, "Isolated modular multilevel DC-DC converter with DC fault current control capability based on current-fed dual active bridge for MVDC application," *IEEE Trans. Power Electron.*, early access.

[2] Y. Chen, S. Zhao, Z. Li, X. Wei and Y. Kang, "Modeling and control of the isolated DC–DC modular multilevel converter for electric ship medium voltage direct current power system," *IEEE J. Emerg. Sel. Topics Power Electron.*, vol. 5, no. 1, pp. 124-139, March 2017.

[3] R. Xie, Y. Shi, and H. Li, "Modular multilevel DAB (M2DAB) converter for shipboard MVDC system with fault protection and ride-through capability," in *Proc. 2015 IEEE Electric Ship Technologies Symp.*, Alexandria, VA, 2015, pp. 427-432.

[4] S. Kenzelmann, A. Rufer, D. Dujic, F. Canales, and Y. R. De Novaes, "Isolated DC/DC structure based on modular multilevel converter," *IEEE Trans. Power Electron.*, vol. 30, no. 1, pp. 89–98, Jan. 2015.

[5] Z. Xing, X. Ruan, H. You, X. Yang, D. Yao, and C. Yuan, "Soft switching operation of isolated modular DC/DC converters for application in HVDC grids," *IEEE Trans. Power Electron*., vol. 31, no. 4, pp. 2753–2766, Apr. 2016.

[6] B. Zhao, Q. Song, J. Li, Y. Wang, and W. Liu, "Modular multilevel high-frequency-link dc transformer based on dual active phase-shift principle for medium-voltage dc power distribution application," *IEEE Trans. Power Electron.*, vol. 32, no. 3, pp. 1779-1791, Mar. 2017.

[7] K. Ilves, S. Norrga, L. Harnefors, and H. -P. Nee, "On energy storage requirements in modular multilevel converters," *IEEE Trans. Power Electron*., vol. 29, no. 1, pp. 77–88, Jan. 2014.

[8] Q. Tu, Z. Xu, H. Huang, and J. Zhang, "Parameter design principle of the arm inductor in modular multilevel converter based HVDC," in *Proc. Int. Conf. Power Syst. Technol*., Hangzhou, China, 2010, pp. 1-6.